

Experimental investigation of double-diffusive groundwater fingers

By PAUL T. IMHOFF

Department of Civil Engineering, Princeton University, Princeton, NJ 08544, USA

AND THEODORE GREEN

Department of Civil and Environmental Engineering, University of Wisconsin,
Madison, WI 53706, USA

(Received 29 July 1986 and in revised form 17 August 1987)

Using a sand-tank model and the salt-sugar system, double-diffusive fingers formed in a saturated porous medium. In contrast to the quasi-steady fingering typically observed in a viscous fluid, the fingering here was quite unsteady. The fingers' structure was observed, and measurements of the sugar flux indicate that double-diffusive groundwater fingers can transport solutes at rates as much as two orders of magnitude larger than those associated with molecular diffusion in motionless groundwater. The buoyancy-flux ratio, $r = \alpha F_T / \beta F_S$, increased from $r = 0.65 \pm 0.02$ (at $R_\rho = 1.02$) to $r = 0.81 \pm 0.06$ (at $R_\rho = 1.50$), where R_ρ is the density-anomaly ratio. (Using the salt-sugar system in a viscous fluid, r was previously shown to decrease with increasing R_ρ .) The buoyancy flux due to sugar varied approximately as $R_\rho^{-5.6}$, which is almost identical with the variation found for salt-sugar fingers in a viscous fluid. The model of Green (1984) was applied to the experiments and predicted buoyancy-flux ratios and finger widths that were in fairly good agreement with the measured values, although the predicted buoyancy fluxes due to sugar were significantly larger than the measured fluxes.

1. Introduction

In the past few years, concern over groundwater contamination has increased sharply. Vertical contaminant transport in groundwater due to buoyancy-driven motions may be important in many situations. One such mechanism, which relies on the gravitational potential energy of the system, is double-diffusive groundwater fingering. This mechanism may occur in the situation where warm, chemically laden, 'salty' groundwater overlies cooler, fresher, and denser groundwater. Although not yet observed in natural groundwater, this mechanism has been found to be important in the vertical transport of salt in the ocean (Turner 1985). Two requirements for the formation of fingers are (i) the fluid must contain at least two components with different molecular diffusivities, and (ii) the faster diffusing component must be stabilizing and the slower diffusing component destabilizing to the vertical density gradient.

In a porous medium a significant amount of theoretical work has already been done to study double-diffusive fingering, as well as a similar double-diffusive process which results in a 'diffusive' configuration. (Here, the faster diffusing component is destabilizing and the slower diffusing component stabilizing to the vertical density gradient.) An analysis for the onset of double-diffusive convection was first

performed by Nield (1968) and then extended by Taunton, Lightfoot & Green (1972). Tyvand (1980) extended the analysis to an anisotropic porous medium. Green (1984) applied a model successful in describing fingers in the ocean to fully developed fingers in groundwater.

Experimental work was performed by Taylor & Veronis (1986) who used a Hele-Shaw cell to study double-diffusive fingering. In the early part of their experiments, the horizontal scale of the fingers is small in comparison to the plate spacing, and the Hele-Shaw cell breaks down as a model for groundwater fingers. However, the model is much better at the end of their experiments, when the horizontal scale of the fingers is approximately 8 times the plate spacing.

The only experimental work on double-diffusive convection in a porous medium was performed by Griffiths (1981), who used both a Hele-Shaw cell and a sand-tank model to study the 'diffusive' configuration. His results were able to explain several characteristics of the Wairakei geothermal system.

There is a noticeable lack of experimental work for double-diffusive groundwater fingering in a porous medium, where dispersion could easily disrupt the coherent fingering pattern. The main justification for the present study was the lack of evidence for the existence, let alone the importance, of this transport mechanism.

2. Experimental investigation

2.1. Objective and scope

The goals of this investigation were threefold: to determine if double-diffusive groundwater fingers can form in a saturated porous medium; to observe the fingers' structure and growth rate; and to measure the fluxes of dissolved substances associated with this transport mechanism. Three types of experiments were performed: visualization experiments, where the fingers' structure and growth rate were observed; flux experiments, where measurements were made of the fluxes of dissolved substances associated with the fingers; and one experiment where a negatively buoyant contaminant element was introduced into a saturated, stratified porous medium to test the starting conditions for the visualization and flux experiments and to better model the formation of double-diffusive groundwater fingers in nature. Several preliminary experiments were also performed.

2.2. The preliminary experiments

In all experiments sugar (sucrose) and salt (sodium chloride) were used as the two substances in the double-diffusive mechanism. The salt-sugar system was chosen over the more physically realistic salt-heat system for convenience. Difficulties are sometimes encountered with sidewall heat losses in the salt-heat system.

The salt-sugar system was first used to study double-diffusive fingering by Stern & Turner (1969). Here, sugar replaces salt as the slower diffusing substance, and salt replaces heat as the faster diffusing substance. These systems differ primarily in two ways: first, heat can be conducted through the porous medium while sugar cannot; and secondly, for the fluid phase the molecular diffusivities of heat and salt differ by about a factor of 100, while the molecular diffusivities of sugar and salt differ by about a factor of 3. Thus, for similar concentrations of diffusing substances the fingers observed in the experiments are expected to be much weaker than those occurring in a natural setting, where heat usually is the stabilizing quantity.

Several preliminary experiments were performed using a 250 ml glass beaker and a Plexiglas tank with internal dimensions of 10.0 cm × 0.85 cm × 24.0 cm

(length \times width \times height). Coarse sand was placed in these containers and was saturated with a heavier salt solution in the lower region and with a lighter sugar solution in the upper region. The sugar solution was usually dyed with green food colouring, although in one case the dye was placed in the interface region between the sugar and salt solutions. Although qualitative in nature, the preliminary experiments did show that double-diffusive fingers can form in a saturated porous medium. Unlike the later visualization experiments, these experiments showed the presence of both upward- and downward-moving fingers. Later experiments were designed to show only the presence of downward-moving fingers.

2.3. *The visualization and flux experiments*

2.3.1. *The apparatus*

The Plexiglas apparatus used in both the visualization and flux experiments is shown in figure 1. The actual porous-medium chamber (i.e. the front tank) is 45.7 cm deep with a horizontal area of 1.4 cm \times 24.2 cm. Beneath the front tank is a cylindrical reservoir, which is separated from the front tank by a wire mesh screen with 0.108 mm openings. The wire mesh screen covers a 3.2 mm wide slit centred in the Plexiglas bottom to the front tank. This slit is 22.8 cm long and begins approximately 0.7 cm from either end of the front tank.

A piece of plastic 0.56 mm thick is used to divide the front tank into upper and lower sections, which contained the sugar and salt solutions. This plastic divider fits in a horizontal slit 0.64 mm thick in the front and side walls of the front tank. Along the back wall, the plastic divider is squeezed between two silicone O-rings. The divider is located 20 cm above the bottom of the front tank and is removed to start an experiment.

The back tank of the apparatus is used to keep an equal hydraulic head across the plastic divider so that no fluid leaks around the O-rings from the front to the back tank. Liberal amounts of silicone grease placed on the divider and O-rings served as additional protection against leakage of fluid from the front tank.

2.3.2. *The porous medium*

Glass beads with diameters 90% in the range of 0.500 mm to 0.710 mm were used to make the porous medium. The beads were spherical in shape with not more than 5% irregularly shaped particles. These beads were cleaned and oven dried before each experiment.

At the end of each experiment, the front tank was flushed with water and the intrinsic permeability of the porous medium measured in place. The mean value of the intrinsic permeability for the visualization and flux experiments was $k = 2.57 \times 10^{-6} \text{ cm}^2$, with an estimated standard deviation of $0.11 \times 10^{-6} \text{ cm}^2$ based on 6 measurements (one for each experiment). The porosity of the porous medium was also found from knowing the volume of the front tank, the mass of glass beads added, and the density of glass. The mean value of the porosity for the visualization and flux experiments was $n = 0.39$, with an estimated standard deviation of 0.01, again based on 6 measurements. Even though a new porous medium was created for each experiment (using a fresh batch of clean glass beads), the properties of the porous medium were nearly the same for all experiments.

2.3.3. *Experimental method for the visualization experiments*

Here, the object was to observe the finger structure and to measure the growth rate of the fingers. Three experiments of this type were performed, differing only in the

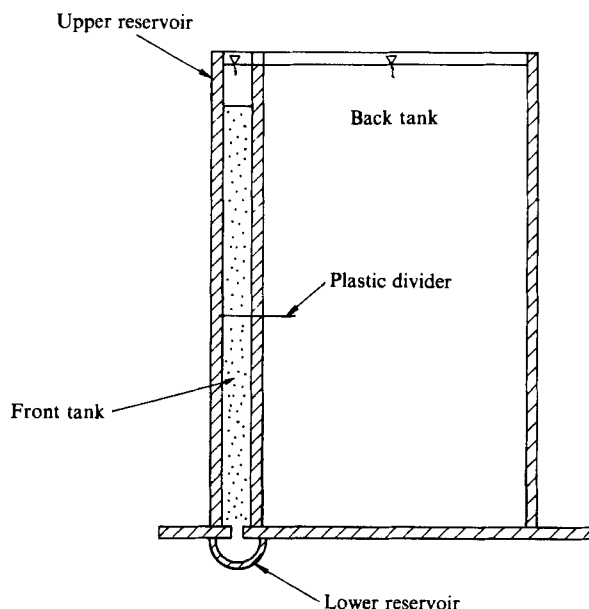


FIGURE 1. Cross-sectional view of the apparatus. Not to scale.

Experiment	Type	ΔS †	ΔT †	Sp. gr.‡ (sugar)	Sp. gr.‡ (salt)
1	Visualization	0.2162	0.1364	1.090	1.099
2	Visualization	0.1712	0.1369	1.070	1.100
3	Visualization	0.2322	0.1371	1.097	1.100
4	Flux	0.2161	0.1371	1.090	1.100
5	Flux	0.2322	0.1371	1.096	1.099
6	Flux	0.1988	0.1371	1.081	1.098
7	Test	0.1712	0.1371	1.070	1.100

† ΔS and ΔT refer to the difference in S (sugar concentration, g of sugar/g of solution) and T (salt concentration, g of salt/g of solution) between the sugar and salt solutions, separated by the plastic divider, at the beginning of each experiment. In the test experiment where the plastic divider was not used, ΔS and ΔT refer to the difference in S and T between the negatively buoyant contaminant element (dyed sugar solution introduced into the upper layer of the porous medium) and the salt solution saturating the lower layer of the porous medium.

‡ Specific gravities of the starting solutions based on the density of water at 20 °C. The specific gravities of the solutions at the same concentration differ because of the different starting temperatures.

TABLE 1. Initial specific gravities and concentrations of sugar and salt solutions

initial sugar concentration. The specific gravities and concentrations of the sugar and salt solutions before the start of each experiment are given in table 1.

After making the sugar and salt solutions, a small amount of fluorescent dye (Lissamine FF) was added to the sugar solution. The weight fraction of the fluorescent dye was less than 0.06 % for all of the visualization experiments. The solutions were then deaired and allowed to come to temperature equilibrium in

the room: that is, the two solutions were at the same temperature although this temperature differed by up to 3 °C from the room temperature.

With the solutions deaired and at temperature equilibrium, the bottom region of the porous medium was formed. The salt solution was added to the front tank and lower reservoir, and glass beads were packed underwater in layers approximately 4 cm thick. Each layer was rodded throughout, while the underlying layer was rodded slightly to eliminate any bridging. Fluid was added incrementally to the back tank to maintain an equal hydraulic head in the front and back tanks.

Once the top of the porous medium was approximately 5 mm below the eventual interface (the location of the above-mentioned slit), the plastic divider was inserted, leaving a thin fluid layer between the top of the porous medium and the underside of the divider. (It was necessary to leave this 5 mm gap in order to allow for the easy insertion of the divider. The glass beads tended to lodge themselves in the slit, hindering the divider's insertion. The influence of this 5 mm gap will be discussed later.) The salt solution above the plastic divider was then siphoned off. Care was taken so that no air bubbles were trapped in the interface region. The top region of the porous medium was then created in the same manner as the bottom region, now using the dyed sugar solution. The top region of the porous medium was made the same depth as the bottom region, with a small layer of dyed sugar solution lying above the top of the porous medium. The front tank was then covered to reduce evaporation.

Each experiment began when the plastic divider was removed. The outside wall of the front tank was then illuminated with four 15 W black light bulbs. Pictures were taken and sketches made of the ensuing dye patterns as the experiment progressed. Each experiment ended when the fingers had grown to the bottom of the front tank.

2.3.4. *Experimental method for the flux experiments*

Here, the object was to measure the fluxes of dissolved substances associated with fingering. Three such experiments were performed, again differing only in the initial sugar concentration. The initial specific gravities and concentrations of the sugar and salt solutions at the start of each experiment are given in table 1. The initial sugar and salt concentrations of two of the three flux experiments were nearly identical with those of two of the visualization experiments.

The procedures used to construct the porous medium and start the experiment were the same as those used in the visualization experiments with one major difference: no dye was added to the sugar solution. In addition, the amount of sugar solution above the porous medium was made as large as possible, forming an upper reservoir from which many samples could be taken.

Again, each experiment was started by removing the plastic divider separating the upper and lower regions. From the upper reservoir of fluid above the top of the porous medium, 5 ml samples were then removed at time intervals ranging from $\frac{1}{2}$ h to 24 h, depending on the initial concentrations and the time after the interface was removed. The fluid in the upper reservoir was mixed well with a glass rod before removing each sample. Between the removal of samples, the front tank was covered to reduce evaporation. After the last sample was removed from the upper reservoir, the fluid in the lower reservoir was mixed using a magnetic stirrer, and a sample removed from it. The removal of this sample from the lower reservoir marked the end of the experiment.

It would have been desirable to remove fluid samples from the lower reservoir

throughout each experiment, just as was done for the upper reservoir. However, removing samples of the needed size from this small lower reservoir would have induced an artificial downward flux of the sugar solution, significantly influencing the flux measurements.

2.3.5. *Analysis of the samples*

For each sample the optical rotation was measured to an accuracy of 0.2% (at 20.0 °C within ± 0.2 °C) using a Perkin Elmer Model 141 Polarimeter. The density of each sample was measured to an accuracy of 2.5×10^{-4} g/cm³ (at 25.00 °C within ± 0.04 °C) using a Mettler/Parar precision density meter, model DMA 10. The sodium chloride concentration T and sucrose concentration S (in grams of solute per gram of solution) were then found by inverting the polynomials of Ruddick & Shirlcliffe (1979). The computed S had an estimated standard error of 0.00005, based on the analysis of 10 samples removed from a standard solution, and a possible bias of +0.0003. The computed T had an estimated standard error of 0.00010, based on the analysis of 10 samples removed from a standard solution, and a possible bias of -0.0003. Although these accuracies were realized in experiments 5 and 6, in experiment 4 the estimated standard error of the computed S and T was larger: 0.00050 based on the analysis of 7 samples removed from a standard solution. However, the possible bias in the computation of S and T for experiment 4 was the same as that reported above.

2.4. *A test experiment*

The starting conditions for both the visualization and flux experiments were somewhat artificial. When each experiment was started, a plastic divider which had separated the upper and lower regions of the porous medium was removed. The upper region of the porous medium then fell approximately 5 mm before coming into contact with the lower region. To test the influence of these starting conditions on the experimental results, a test experiment was performed (experiment 7). A negatively buoyant contaminant element (dyed sugar solution) was introduced into the upper porous medium, which was saturated with fresh water. The lower layer of the porous medium was saturated with a salt solution, which was denser than the dyed sugar solution. Because no divider was removed, the starting conditions for this experiment better reproduce the probable starting conditions for double-diffusive groundwater fingers in nature. There, warm, contaminated groundwater may descend quickly through the saturated zone until it encounters a lower layer of colder and heavier water.

To set up this experiment, a salt solution, a dyed sugar solution, and a volume of deionized water were deaired and allowed to reach temperature equilibrium. Again, the weight fraction of the fluorescent dye in the sugar solution was less than 0.06%. (See table 1 for the initial specific gravities and salt-sugar concentrations of the solutions.) Using the salt solution, the bottom region of the porous medium was made, using the same glass beads and following the same procedures as in the earlier experiments. When the porous-medium level was at the height of the slit, the excess salt solution was siphoned off, leaving only a thin film of fluid covering the top of the porous medium. Fresh deionized water was then slowly added to the front tank by letting it impact a piece of foam rubber. This reduced the mixing of the fresh water and the underlying salt solution. The upper region of the porous medium was then created using more beads and deionized water, following the same procedures as before. The plastic divider was never inserted in the front tank.

When the top of the porous medium was approximately 5 cm above the slit, a small Plexiglas box with an attached feed line was inserted in the middle of the front tank. The porous medium was then formed around the Plexiglas box and feed line following the earlier procedures. (The box cancelled any initial vertical momentum of the dyed sugar solution associated with its introduction.) After finishing creating the upper region of the porous medium, the front tank was covered to reduce evaporation.

The experiment was started by opening the feed line and allowing 39 ml of dyed sugar solution to enter the upper porous medium and strike the Plexiglas box. The box diverted the flow to the sides, and the sugar solution (denser than the surrounding fresh water) descended quickly to the interface region between the salt solution and the fresh water. Since the dyed sugar solution was less dense than the underlying salt solution, it spread out along the interface between the salt solution and the fresh water. During this time, the apparatus was illuminated with four 15 W black light bulbs, and pictures were taken and sketches made. Fingers then formed as discussed below. The pictures continued to be taken and the sketches made until the fingers reached the bottom of the front tank.

3. Results

3.1. *The visualization experiments*

3.1.1. *Finger structure*

In each of the visualization experiments, the fingers were observed to start very thin and then to grow wider as they grew longer. When the descending fingers reached the bottom of the front tank, the dye mixed with the upward-moving fingers, rendering further measurements impossible. A sequence of photographs showing the finger growth in one experiment is shown in figure 2.

Measurements of the fingers were made from tracings of the outline of the dyed region as it appeared along the outside wall of the front tank. Usually, the downward movement of the fluorescent dye along this wall was in very regular, fingerlike patterns. However, for two of the three visualization experiments there were some isolated regions where the dye did not move in regular patterns. These regions normally occurred in the corners of the front tank. Here, before the experiment started, some of the dyed sugar solution had leaked around the divider. When the divider was removed, the dyed fluid in these regions moved quickly down the wall in wide streams that were not characteristic of a typical finger. These isolated streams were excluded from the measurements for the finger structure and descent rate.

Two parameters were used to describe the finger structure: the mean finger width; and the mean finger length. The mean finger width was determined by finding the average distance between the centrelines of adjacent, downward-moving fingers and dividing this value by two. The corresponding mean finger length was computed by averaging the distances from the slit in the front wall to the farthest downward projection of each well-defined finger.

In figure 3, the mean finger width is plotted versus the mean finger length for all three experiments. The mean finger width increased significantly from the beginning to the end of each experiment. This widening of fingers was also observed in experiments by Taylor & Veronis (1986) and is discussed further below.

Although the measurements of the finger width and length were made along the

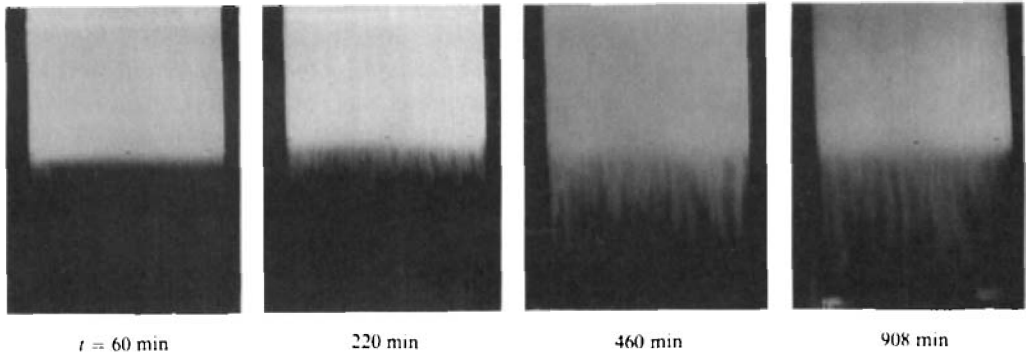


FIGURE 2. A series of pictures of the finger growth in experiment 2. The dyed sugar solution (light coloured fluid) overlies the heavier salt solution. At time $t = 0$, the plastic divider separating the sugar and salt solutions is removed. The width of the dyed region at the top of each picture is 24.2 cm. See table 1 for the solute concentrations and the specific gravities of the starting solutions.

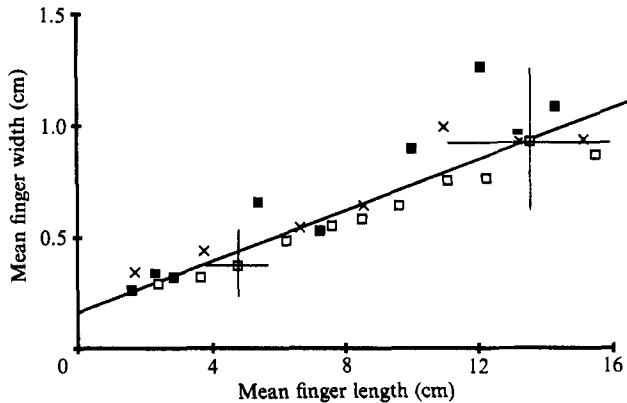


FIGURE 3. The mean finger width as a function of mean finger length: \times , experiment 1; \square , experiment 2; \blacksquare , experiment 3. A linear regression gives the fitted line with slope 0.056. Error bars represent ± 1 estimated standard deviation and are representative for the data.

outside wall of the front tank, the fingers were also visible along the back wall of the front tank. Even though it was impossible to make accurate measurements along the back wall, two conclusions can be made from the observations there: the general structure of the fingers observed along the back wall was the same as that of the fingers observed along the front wall; and the fingers descended about 15% faster along the back wall than along the front wall. Because the measured finger widths were always less than the thickness of the front tank, it seems unlikely that the fingers observed along the front wall were the same fingers that were observed along the back wall.

3.1.2. Finger descent rate

The fingers were observed to descend at a constant rate until they reached the bottom of the front tank. This descent rate differed, though, between experiments. A regression analysis was used to fit a line to the data relating the finger length to time for each experiment. The slope of each fitted line is the finger descent rate, which is shown with the initial density-anomaly ratio, $R_\rho = \bar{\alpha}\Delta T/\bar{\beta}\Delta S$, in table 2. Here, $\alpha = \rho^{-1}\partial\rho/\partial T$ and $\beta = \rho^{-1}\partial\rho/\partial S$ are evaluated at the average values of the sugar and salt concentrations ($\bar{\alpha} = \alpha(\bar{T}, \bar{S})$, $\bar{\beta} = \beta(\bar{T}, \bar{S})$) of the two fluid layers

Experiment	R_ρ	Finger descent rate (cm/h)
3	1.023	2.94 ± 0.10 SE based on 10 data points
1	1.094	2.26 ± 0.03 SE based on 10 data points
2	1.390	1.21 ± 0.01 SE based on 14 data points

TABLE 2. Initial density-anomaly ratio and the finger descent rate. Note: SE refers to one estimated standard error.

separated by fingers. The polynomials of Ruddick & Shirtcliffe (1979) were used to compute α and β . Also, ΔS is the difference in sugar concentration, and ΔT is the difference in salt concentration between the same two fluid layers.

The descent rate decreases with increasing R_ρ . This is to be expected, as the driving force due to the sugar is weaker as R_ρ increases. R_ρ should have remained constant during each visualization experiment, since the fingers were still growing longer and should not yet have begun to transport sugar or salt beyond their farthest vertical extent. In the flux experiments reported later, R_ρ changed during the measurement period.

It is reasonable to assume that the fluid velocity in the fingers (the average interstitial velocity) is more or less the same as the finger descent rate, since there were not large accumulations of dye at the tips of the fingers. Converting the finger descent rates (average interstitial velocities) to Darcy velocities gives velocities which range between 0.1 m/day and 0.3 m/day. According to Todd (1980), typical groundwater velocities range between 2 m/yr and 2 m/day. Thus, the observed velocities due to the double-diffusive fingers in the laboratory experiments are large when compared to typical values. Actual finger descent rates in a natural setting, though, are likely to be smaller since ΔS and ΔT are then probably much smaller.

3.2. The flux experiments

3.2.1. Sugar flux

It was impossible to observe the fingers in the flux experiments. Based on the visualization experiments, it was assumed that the fingers grew to the top and bottom of the porous medium and remained at this length for the duration of each experiment.

Both the downward sugar flux out of and the upward salt flux into the upper reservoir were computed from the changes in sugar concentration and salt concentration of the fluid in the upper reservoir between successive sampling times. The sugar flux was computed using

$$F_s = \rho H \frac{\delta S}{\delta t}, \quad (1)$$

where F_s is the sugar flux in grams of sugar $\text{cm}^{-2} \text{s}^{-1}$, ρ is the mean value of the fluid density in the upper reservoir between successive sampling times, H is the depth of fluid in the upper reservoir (which decreased over time because of the sampling), and δS is the absolute value of the change in S between samples that were withdrawn at time intervals δt apart†. The salt flux F_T was computed using a similar equation.

† F_s was also computed using $F_s = H \delta(\rho S)/\delta t$ and F_T using a similar equation (Imhoff 1985). However, the difference between computing the fluxes with these equations and with the equations above is small: the computed fluxes almost always differ by less than 3%.

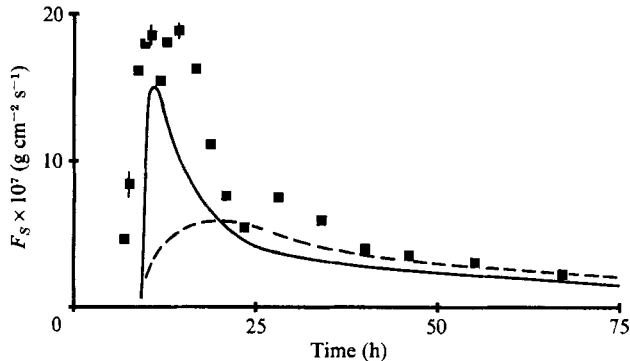


FIGURE 4. The sugar flux, F_S (equation (1)), out of the upper reservoir as a function of time after the start of the experiment: —, experiment 4; ■, experiment 5; ----, experiment 6. Error bars represent ± 1 estimated standard error and are representative for the data points shown. (The first few computed fluxes for experiment 5 are not shown because of the large random error associated with these values.)

F_S for experiment 5 is plotted versus time in figure 4. A sharp peak in the sugar flux occurs approximately 12 h after the start of the experiment, when (presumably) all of the fingers have reached the upper reservoir. The flux then decreases in magnitude as the experiment runs down. The peak value of F_T occurs at approximately the same time as the peak value of F_S (Imhoff 1985). Curves representing the change in F_S versus time for experiments 4 and 6 are also shown in figure 4. For these experiments as well, the peak value of F_T occurs at approximately the same time as the peak value of F_S .

It is interesting to compare F_S with the sugar flux that would occur if the only transport mechanism was molecular diffusion. An estimate for the sugar flux due to only molecular diffusion comes from the following very approximate equation

$$F_{Sm} = \frac{2}{3} K_S n \frac{\Delta(\rho S)}{L}, \quad (2)$$

where F_{Sm} is the flux of S due to molecular diffusion ($\text{g cm}^{-2} \text{s}^{-1}$), $\frac{2}{3}$ is the approximate value for the tortuosity of paths in beds of glass beads (Saffman 1960), K_S is the molecular diffusivity of sugar† (taken as $0.5 \times 10^{-5} \text{ cm}^2 \text{ s}^{-1}$), $\Delta(\rho S)$ is the difference in ρS between the upper and lower reservoirs, and L is the total height of the porous medium. Equation (2) was evaluated for the time when the fingers had just grown to the top and bottom of the porous medium. Implicit in this equation is the assumption that ρS varies linearly between the upper and lower reservoirs.

The peak value of F_S in experiment 5 is approximately 200 times larger than F_{Sm} , the largest difference between F_S and F_{Sm} for the three flux experiments. Thus, the fluxes of dissolved substances associated with double-diffusive fingering can be much larger than those associated with molecular diffusion in motionless groundwater.

The sugar flux due to molecular diffusion was also computed based on the actual starting conditions for the experiments (a sharp interface between a concentrated sugar solution and a salt solution with no sugar), using the solution for the analogous heat-conduction problem (Carslaw & Jaeger 1959). At the time when the peak sugar

† The value for K_S is approximate and was taken from Weast (1983).

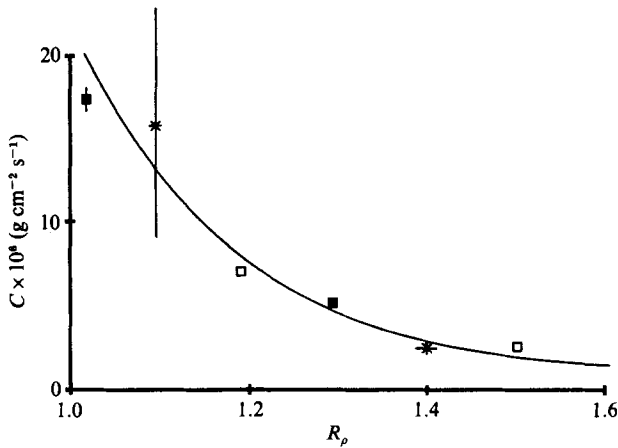


FIGURE 5. The buoyancy-flux coefficient for sugar, C (equation (4)), as a function of the density-anomaly ratio, $R_\rho = \bar{\alpha}\Delta T\bar{\beta}\Delta S$: \times , experiment 4; \blacksquare , experiment 5; \square , experiment 6. The fitted curve is $C = 2.1 \times 10^{-5}R_\rho^{-5.6}$ ($\text{g cm}^{-2} \text{s}^{-1}$). Error bars represent ± 1 estimated standard error and most are so small as not to appear. Only one point has a significant error.

flux due to fingers occurred, there still would be essentially no sugar flux out of the upper reservoir associated with molecular diffusion.

3.2.2. Sugar buoyancy flux

The buoyancy flux due to sugar βF_S ($\text{g cm}^{-2} \text{s}^{-1}$) is also of interest. Based on dimensional arguments (Turner 1965) and experimental work (Stern & Turner 1969; Lambert & Demenkow 1972; and Griffiths & Ruddick 1980), the flux law for viscous-fluid fingers takes the form

$$\beta F_S = C(\beta\Delta S)^{\frac{4}{3}}. \tag{3}$$

(Here, ‘viscous fluid’ refers to water, as opposed to water in a porous medium.) For viscous-fluid fingers $C = C(R_\rho, \tau, \nu/K_T)$, where $\tau = K_S/K_T$, ν is the kinematic viscosity, and K_T is the molecular diffusivity of salt. It seems reasonable to hypothesize a similar flux law for groundwater fingers, where now $C = C(R_\rho, \tau, \nu/K_T, k, n)$. This flux law was investigated for the three flux experiments, keeping all the parameters that may affect C constant except for R_ρ . Using (1) and (3), C was determined from

$$C = \overline{\rho\beta}H(\bar{\beta}\Delta S)^{-\frac{4}{3}}\frac{\delta S}{\delta t}, \tag{4}$$

where $\overline{\rho\beta} = \rho\beta(\bar{T}, \bar{S})$ and $\bar{\beta} = \beta(\bar{T}, \bar{S})$. C is plotted versus R_ρ in figure 5. The data are sparse because R_ρ and ΔS could only be determined at the beginning and end of each experiment. (Only at these times were the values of S and T known in the lower reservoir.) C varies quite rapidly with R_ρ when R_ρ is small, and much less for larger values. A regression analysis gives

$$C = 2.1 \times 10^{-5}R_\rho^{-5.6}. \tag{5}$$

It should be emphasized that the $\frac{4}{3}$ power law given in (3) was not tested here. There was insufficient data to do this. Instead, the $\frac{4}{3}$ power law was assumed correct and the relationship between C and R_ρ determined for comparison with a similar relationship for viscous-fluid fingers.

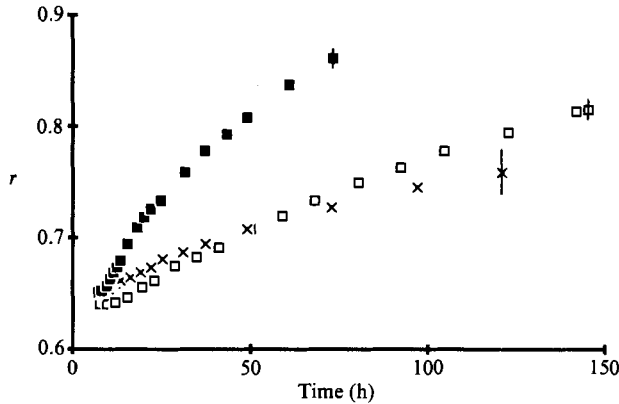


FIGURE 6. The buoyancy-flux ratio, r (equation (6)), as a function of time after the start of the experiment: \times , experiment 4; \blacksquare , experiment 5; \square , experiment 6. Error bars represent ± 1 estimated standard error and are representative for the data.

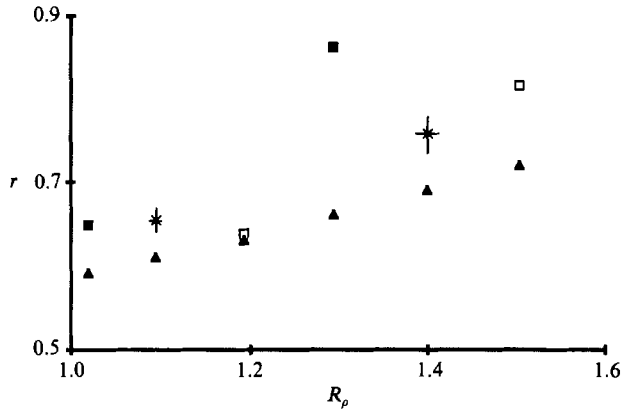


FIGURE 7. The buoyancy-flux ratio, r (equation (6)), as a function of the density-anomaly ratio, $R_p = \alpha\Delta T/\bar{\beta}\Delta S$: \times , experiment 4; \blacksquare , experiment 5; \square , experiment 6; \blacktriangle , Green's model. Error bars represent ± 1 estimated standard error, and most are so small as not to appear.

3.2.3. Buoyancy-flux ratio

The buoyancy-flux ratio, $r = \alpha F_T/\beta F_S$, is a measure of the ability of the fingers to change the densities of fluid layers separated by fingers. Here, αF_T is the buoyancy flux due to salt. This flux ratio was computed from the upper-reservoir data using the relation derived by Griffiths & Ruddick (1980)

$$1 - r = \frac{1}{\rho\beta} \frac{d\rho}{dS}. \quad (6)$$

An equation of the form $\rho = a + bS + cS^2$ was fitted to the upper-reservoir data. From this equation, the slope $d\rho/dS$ was computed at each sampling time, when ρ and β were also known. This gave r at each sampling time, as shown in figure 6. Here, r increases with time, while for salt-sugar fingers in a viscous fluid Griffiths & Ruddick (1980) found that r decreased as each experiment ran down. The overall situation for the viscous-fluid fingers, though, was different from that observed in these experiments. This is discussed below.

The buoyancy-flux ratio is plotted against R_p in figure 7. Again, the lack of data

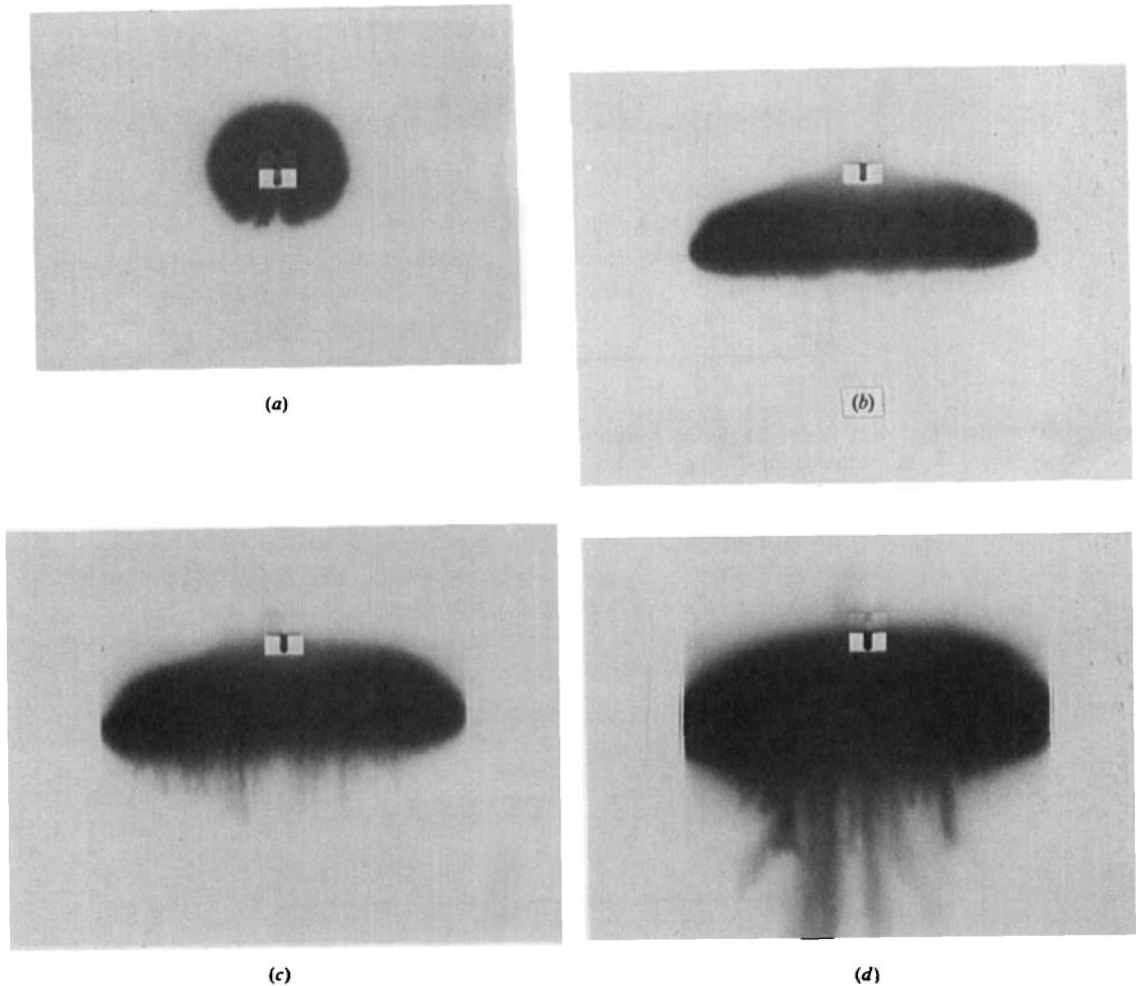


FIGURE 8. A series of pictures of the finger growth in experiment 7. The dyed sugar solution (dark fluid) is introduced with the device that appears as a white rectangle with a dark centre on the figure (described as 'the Plexiglas box' in the text) into the upper region of the porous medium, which is saturated with fresh water. The bottom of the Plexiglas box is approximately 5 cm above the fresh water/salt water interface. The dyed sugar solution is heavier than the surrounding fresh water and lighter than the underlying salt water. The pictures are at times (after injecting the sugar solution) (a) 0; (b) 38 min; (c) 205 min; and (d) 807 min. The maximum width of the dyed region in pictures (c) and (d) is 24.2 cm. See table 1 for the solute concentrations and the specific gravities of the starting solutions.

results from knowing the value of R_p only at the beginning and end of each experiment. The data point for the end of experiment 5 falls far outside the trend of the other data points in this figure. No reasonable explanation has been found for this.

3.3. A test experiment

The experiment involving the negatively buoyant contaminant element (experiment 7) served two purposes: (i) it tested the influence of the starting conditions for the other experiments; and (ii) it better modelled the formation of double-diffusive groundwater fingers in a natural setting. A sequence of photographs showing the descent of the dyed sugar solution and the progression of finger growth for this experiment is shown in figure 8.

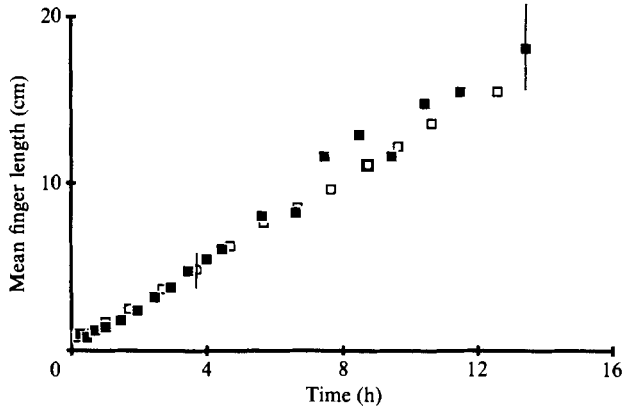


FIGURE 9. The mean finger length as a function of time after the start of the experiment: \square , experiment 2; \blacksquare , experiment 7. Error bars represent ± 1 estimated standard deviation and are representative for the data.

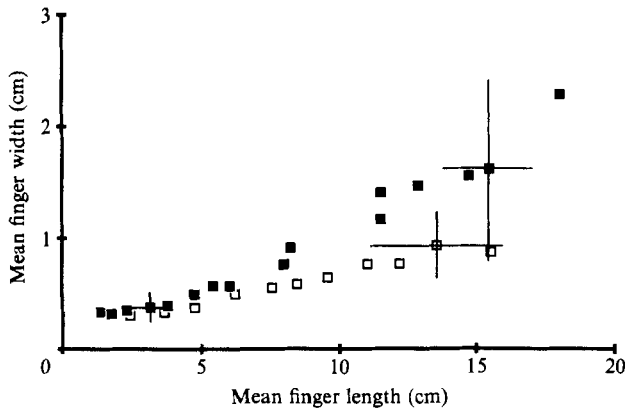


FIGURE 10. The mean finger width as a function of mean finger length: \square , experiment 2; \blacksquare , experiment 7. Error bars represent ± 1 estimated standard deviation and are representative for the data.

The initial concentrations of the sugar and salt solutions used in experiment 7 were nearly identical with those used in experiment 2, a visualization experiment. However, in experiment 7, as the dyed sugar solution descended to the interface between the fresh water and salt water, the sugar solution mixed with the surrounding fresh water and decreased the initial value of S . Thus, the value of S when the dyed sugar solution contacted the denser salt solution is somewhat smaller than that in experiment 2.

In figure 9, the mean finger length is plotted versus time for experiments 2 and 7. The finger lengths reported for experiment 7 are for the fingers in the centre of the front tank, where the sugar concentration of the dyed region should be closest to the sugar concentration used in experiment 2. The descent rates of the fingers for experiments 2 and 7 are nearly the same. Linear regressions yield a descent rate of $1.21 \pm 0.01\text{SE cm/h}$ (based on 14 data points) for experiment 2 and $1.35 \pm 0.03\text{SE cm/h}$ (based on 20 data points) for experiment 7. (SE refers to one estimated standard error.)

Another comparison can be made between experiments 2 and 7. The mean finger

width is plotted against the mean finger length for each of these experiments in figure 10. As before, the fingers reported for experiment 7 are those in the centre of the front tank. The finger widths for experiment 7 are larger than the corresponding finger widths for experiment 2, especially when the fingers are very long. This difference is attributed to the fact that as the fingers grew longer in experiment 7, there were no bounding fingers on the sides to limit the lateral finger growth.

The widening of the fingers observed in the visualization experiments and in the test experiment needs additional explanation. In all experiments, it was impossible to follow any one finger as it grew from the interface to the bottom of the apparatus. As the fingers grew longer, they appeared to merge together, forming wider fingers in which their original identity was lost. Although this behaviour is difficult to describe precisely, it did occur in both the visualization experiments and in the test experiment.

Based on this comparison of results between experiments 2 and 7, it seems that the starting conditions did not have a significant effect on the double-diffusive mechanism or on the fluxes.

4. Discussion

4.1. Comparisons between the visualization and the flux experiments

Consider experiments 1 and 4, and 3 and 5. In both sets of experiments, the starting conditions were almost identical (see table 1).

From experiments 1 and 3, it is possible to estimate the downward sugar flux based on the observed finger descent rate. These sugar fluxes were computed assuming that the sugar concentration in the fingers was the same as the initial sugar concentration of the upper-layer fluid. The downward-moving fingers were also assumed to occupy one half of the porous medium, the other half being occupied by upward-moving fingers. With these assumptions, the sugar flux was estimated from

$$F_S = \frac{1}{2}nUS_u\rho_u, \quad (7)$$

where U is the finger descent rate (which was found to be quite constant in each visualization experiment), S_u is the initial sugar concentration of the upper-layer fluid, and ρ_u is the initial density of the upper-layer fluid. The estimated sugar fluxes from experiments 1 and 3 were approximately 20 times greater than the peak sugar fluxes measured in the corresponding flux experiments. This implies that the sugar concentration in the tips of the descending fingers is much smaller than the initial sugar concentration of the upper-layer fluid.

Now consider the time of arrival of the fingers at the top and bottom of the porous medium. These two times should be identical if the fingers grow upward and downward at the same rate. In experiments 1 and 3, the fingers were assumed to have reached the bottom of the porous medium when the dyed fingers (as viewed from the outside wall) arrived there. In experiments 4 and 5, the fingers were assumed to have reached the top of the porous medium when there were measurable changes in the sugar and salt concentration of the fluid in the upper reservoir. (Note that it was impossible to measure the arrival time of the fingers at both the top and bottom of the porous medium for the same experiment.) Using these criteria, the fingers arrived at the bottom of the porous medium approximately 2.4 h earlier than they did at the top of the porous medium for both sets of experiments. Since the time for the fingers to descend to the bottom of the porous medium was 8.7 h for experiment 1 and

5.7 h for experiment 3, this time difference is large. One possible explanation is that since the dye was a third diffusing substance it may have affected the double-diffusive mechanism, although the dye's contribution to the fluid density was negligible. However, this was the only indication that the dye may have affected the results.

A second, more plausible explanation is that the different viscosities of the sugar and salt solutions resulted in different velocities for the upward- and downward-moving fingers. The viscosities of the salt solutions used here were about 60% that of the sugar solutions.

4.2. *Dispersion*

Because of the importance of dispersion in solute transport in a porous medium, some discussion of the transverse and longitudinal dispersion is called for. The parameter commonly used in the analysis of dispersion is the Péclet number, $Pe = Vd/K$, where V is the average interstitial velocity, d is the mean particle diameter, and K is the molecular diffusivity. As mentioned above, it seems reasonable to assume that the fluid velocity V in the fingers is approximately equal to the finger descent rate, since there were no large accumulations of dye at the tips of the fingers in the visualization experiments. Using the measured finger descent rates for V , the Péclet numbers for salt ranged between 1.3 and 3.3, while the Péclet numbers for sugar ranged between 4.1 and 9.9. These values are representative for the early part of all the experiments, when the fingers had not yet reached the bottom of the porous medium. For these Péclet numbers, both molecular diffusion and mechanical dispersion are important in the longitudinal and transverse directions (Fried 1975). Thus, it may be necessary to consider mechanical dispersion in any model for the double-diffusive fingering observed in these experiments. However, in a natural setting with smaller ΔS and ΔT , mechanical dispersion should be less important.

4.3. *Comparison with the salt-sugar fingers in a viscous fluid*

Much previous experimental work investigating double-diffusive fingering has been performed in a viscous fluid using the salt-sugar system. It is worthwhile to make some comparisons between those results and the results from the present investigation.

With the salt-sugar system in a viscous fluid, a thin fingering region typically separates two turbulent, well-mixed convecting regions. Once formed, the fingering region is quasi-steady, varying only on the longer timescale of the rundown of layer properties. This was reported by Stern & Turner (1969), Lambert & Demenkow (1972), and Griffiths & Ruddick (1980), among others. In a porous medium, though, there were no observed convecting regions in experiments on a similar vertical scale, and with similar density-anomaly ratios and salt-sugar concentrations. The fingers were unsteady and continued to grow until they reached the bottom of the porous medium. Finger growth was stopped by the physical dimensions of the tank. It is possible that a larger apparatus would have indeed showed well-mixed regions separated by a very thick fingering interface. Further work is required to investigate this possibility.

Because the overall situation is so different in our porous-medium experiments, it is difficult to make meaningful comparisons between fingering here and that in a viscous fluid. Nevertheless, comparisons will be made to highlight the differences and similarities between the two situations.

First, the finger structure in a porous medium is very different from that in a viscous fluid. For salt-sugar fingers in a viscous fluid, Shirtcliffe & Turner (1970)

found that the finger widths were typically in the range from 0.04 cm to 0.10 cm, for density-anomaly ratios and salt-sugar concentrations very similar to those used in this study. In the present experiments, the finger widths ranged from 0.3 cm to 1.0 cm, a factor of 10 larger (figure 3).

Assuming the $\frac{4}{3}$ power law for the buoyancy flux is correct, the buoyancy-flux law seems very similar in the viscous-fluid and porous-medium experiments. Griffiths & Ruddick (1980) used the same form of the law as was used in this study (equation (3)) and found the buoyancy-flux coefficient for sugar to be

$$C = 5.5 \times 10^{-3} R_\rho^{-6} \text{ (g cm}^{-2} \text{ s}^{-1}\text{)}. \quad (8)$$

In this study C was found to vary with R_ρ to the -5.6 power. Although the sugar fluxes in a porous medium are two orders of magnitude smaller than the corresponding fluxes in a viscous fluid (as reported by Griffiths & Ruddick), the dependence on the density-anomaly ratio is almost identical.

Finally, there are significant differences between the buoyancy-flux ratios in a viscous fluid and in a porous medium. In a viscous fluid, Griffiths & Ruddick (1980) found that r decreased from $r \approx 0.94 \pm 0.01$ (at $R_\rho = 1.02$) to $r = 0.88 \pm 0.01$ (at $R_\rho = 2$). In a porous medium, the flux ratio increased from $r = 0.65 \pm 0.02$ (at $R_\rho = 1.02$) to $r = 0.81 \pm 0.06$ (at $R_\rho = 1.50$). In addition, there is a much larger variation of r in a porous medium than in a viscous fluid.

4.4. Comparison with a model

It is interesting to compare the present results with the model for double-diffusive groundwater fingers of Green (1984). This quasi-steady model assumes a fingering interface between two well-mixed regions. Although this situation was not observed in our experiments, it is worthwhile to make comparisons between measured results and predictions from this model for the buoyancy-flux ratio, the finger width, and the buoyancy flux due to sugar.

In order to use this model, $\langle T \rangle_z$ and $\langle S \rangle_z$ (the vertical gradients of the horizontally averaged values of S and T) had to be estimated. Because of the lack of data, $\langle S \rangle$ and $\langle T \rangle$ (the horizontally averaged values) were assumed to vary linearly between the upper and lower reservoirs, which seems reasonable for the situation when the fingers had grown to the entire height of the porous medium. With this assumption, $\langle S \rangle_z$ and $\langle T \rangle_z$ were calculated at the times when the fingers first reach the upper and lower reservoirs and at the end of the experiment. (It is only at these times that S and T were known in both the upper and lower reservoirs.) Using these values of $\langle S \rangle_z$ and $\langle T \rangle_z$, Green's model predicts buoyancy-flux ratios that are consistently smaller than the experimental values (figure 7). However, the difference between the measured and predicted r is usually small and is always less than 23%.

The finger width was also computed from the model, assuming that the fingers were square in planform, and using the same values of $\langle S \rangle_z$ and $\langle T \rangle_z$ as above (for the time when the fingers just reach the bottom of the porous medium). The model gives finger widths that are smaller than the measured values by at most 30%. If the analysis is performed when the fingers are very short, the finger widths given by the model agree much better with the measured values. (In this case, $\langle S \rangle_z$ and $\langle T \rangle_z$ are computed by assuming that $\langle S \rangle$ and $\langle T \rangle$ vary linearly over the total finger length. Above and below the fingering region, the solute concentrations are assumed to be the same as the concentrations in the upper and lower reservoirs.) For example, when the descending fingers are 2.5 cm below the slit in the front wall (the total finger

length is assumed to be 5 cm), Green's model gives finger widths that differ from the measured values by at most 18%.

Two trends in the experimental results are also correctly predicted by the model. First, r was observed to increase as R_ρ increased. For larger values of R_ρ and smaller values of $\langle S \rangle_z$ and $\langle T \rangle_z$, the model also predicts an increasing r (see figure 7). Secondly, the fingers were observed to grow wider as they grew longer. Here, the value of R_ρ for the two fluid regions separated by the growing fingers should be constant, since the fingers are still growing longer and should not yet have begun to transport sugar or salt beyond their farthest vertical extent. (This is in agreement with the previously mentioned observation that the vertical fluid velocity in the fingers appeared to be about the same as the finger descent rate.) Although R_ρ should be constant as the fingers are growing, the values of $\langle S \rangle_z$ and $\langle T \rangle_z$ are becoming smaller. Using smaller values of $\langle S \rangle_z$ and $\langle T \rangle_z$ for the same R_ρ , Green's model predicts wider fingers just as were observed.

In the steady state, assuming fingers that are square in planform, Green's model leads to the following expression for the buoyancy flux due to sugar:

$$\beta F_S = \frac{Wng\rho(\beta\hat{S})^2}{8A}, \quad (9)$$

where W and A are dimensionless model parameters which are functions of K_S , K_T , ν , α , β , k , n , $\langle S \rangle_z$ and $\langle T \rangle_z$. All parameters in the above expression are known or can be reliably estimated except for \hat{S} , the amplitude of the horizontally varying sugar concentration in the fingering region. An upper bound for \hat{S} is $\frac{1}{2}\Delta S$. Using this value for \hat{S} and the same estimates for $\langle S \rangle_z$ and $\langle T \rangle_z$ as given above yields buoyancy fluxes that are 3-4 orders of magnitude larger than those measured. It seems unlikely that this discrepancy can be explained by any error in the estimation of \hat{S} .

It is worthwhile to consider the influence of the assumed values of $\langle S \rangle_z$ and $\langle T \rangle_z$ on the predictions from Green's model. The values used above are probably lower bounds. If the actual values of $\langle S \rangle_z$ and $\langle T \rangle_z$ were both twice the estimated values, then the predicted r would change by less than 2%, while the predicted finger widths would decrease by roughly a factor of 1.4. However, βF_S would be reduced to values that are only 2 orders of magnitude larger than those measured. Thus, while r and the finger width are not strongly sensitive to these input parameters, βF_S is.

Despite the fairly good agreement between the experimental results and the model (at least for r and the finger width), it is important to reiterate that Green's model is not entirely amenable to the above analysis since it is a quasi-steady model: R_ρ , $\langle S \rangle_z$ and $\langle T \rangle_z$ are assumed to be constant, and the finger geometry does not vary in the vertical. A better model is clearly needed.

4.5. Possible errors

In all of the experiments, there were several possible sources of error which could have influenced the results. One is the wall effect. The porosity along the walls of the front tank is larger than the porosity inside the porous medium: the glass beads are less densely packed along the walls than elsewhere. This may have caused the solute fluxes to be larger than their values for an equivalent porous medium in a natural setting, especially since the distance between the front and back walls of the front tank was only 23 glass-bead diameters. The measurements of the finger structure and descent rate also may have been influenced since these measurements were performed along the outside wall of the front tank.

Another possible error source is the hydraulic connection between the front tank and the lower reservoir. This connection consists of a 3.2 mm wide slit which gives a flow area that is about 80% smaller than the flow area of the front tank. Because of this constriction in the flow between the front tank and the lower reservoir, the slit may have acted as a control in limiting the flux of sugar and salt. This error source exists because when the apparatus was designed, it was not intended to be used as a means of measuring solute fluxes. Only later, when the fingers were found to grow to the height of the porous medium, was this changed.

Several other possible sources of minor error are discussed by Imhoff (1985).

5. Summary

These experiments have shown that double-diffusive groundwater fingers can form in a saturated porous medium. The fingers formed at a sharp interface and grew to the bottom of the porous medium column, with the finger widths increasing from ≈ 0.3 cm when the fingers were short to ≈ 1.0 cm when the fingers were long. The downward sugar flux associated with double-diffusive fingering was as much as 200 times larger than that due to molecular diffusion in motionless groundwater. Thus, fingering could play a major role in the vertical transport of near-surface pollutants in groundwater.

The buoyancy flux due to sugar βF_s was computed in the experiments. Assuming that $\beta F_s = C(\beta \Delta S)^{\frac{4}{3}}$, the buoyancy-flux coefficient C was found to vary strongly with the density-anomaly ratio R_ρ . The power law $C = 2.1 \times 10^{-5} R_\rho^{-5.6}$ fitted the data reasonably well. The flux ratio r increased steadily during each experiment. It also increased over all three experiments from $r = 0.65 \pm 0.02$ (at $R_\rho = 1.02$) to $r = 0.81 \pm 0.06$ (at $R_\rho = 1.50$).

The model of Green (1984) was applied to the experiments and predicted buoyancy-flux ratios and finger widths that were in fairly good agreement with the measured values. However, the predicted buoyancy fluxes due to sugar were significantly larger than the measured fluxes. Green's model also gives a sugar flux dependence on $(\Delta S)^2$ which is in contradiction to the $\frac{4}{3}$ power law assumed above.

Because of the scarcity of data, the $\frac{4}{3}$ power law for the buoyancy flux due to sugar was not tested, and the relations describing the variations of C and r with R_ρ are not firmly established. Also, the influence of the porous-medium properties (e.g. the porosity and the intrinsic permeability) on the fingers was not investigated. Finally, the actual system causing double-diffusive fingering in groundwater will likely involve heat and one (or possibly several) solutes. It is difficult to extrapolate the results from this study to other situations because the dependence of the mechanism on the diffusivity ratio ($\tau = K_S/K_T$) and the Prandtl number ($\sigma = \nu/K_T$) has not been studied. However, based on the investigation of fingering in a viscous fluid, the fingering mechanism in a natural setting involving heat and one or several solutes with similar values of ΔS and ΔT should be more vigorous than the salt-sugar system studied here, i.e. faster descending fingers and larger fluxes. (Smaller values of ΔS and ΔT will obviously lead to weaker fingering.) Further, more extensive, and larger-scale experiments with other porous media are needed to resolve such questions, along with those pertaining to the overall context in which porous-medium fingering occurs.

The authors express their appreciation to an anonymous reviewer whose helpful comments strengthened this work.

REFERENCES

- CARSLAW, H. S. & JAEGER, J. C. 1959 *Conduction of Heat in Solids*, pp. 53–55. Oxford University Press.
- FRIED, J. J. 1975 *Groundwater Pollution*, pp. 29–34. Elsevier.
- GREEN, T. 1984 Scales for double-diffusive fingering in porous media. *Water Resources Res.* **20**, 1225–1229.
- GRIFFITHS, R. W. 1981 Layered double-diffusive convection in porous media. *J. Fluid Mech.* **102**, 221–248.
- GRIFFITHS, R. W. & RUDDICK, B. R. 1980 Accurate fluxes across a salt–sugar finger interface deduced from direct density measurements. *J. Fluid Mech.* **99**, 85–95.
- IMHOFF, P. T. 1985 Experimental investigation of double-diffusive groundwater fingers. M.S. thesis, The University of Wisconsin–Madison.
- LAMBERT, R. B. & DEMENKOW, J. W. 1972 On the vertical transport due to fingers in double diffusive convection. *J. Fluid Mech.* **54**, 627–640.
- NIELD, D. A. 1968 Onset of thermohaline convection in a porous medium. *Water Resources Res.* **4**, 553–560.
- RUDDICK, B. R. & SHIRTCLIFFE, T. G. L. 1979 Data for double diffusers: physical properties of aqueous salt–sugar solutions. *Deep-Sea Res.* **26A**, 775–787.
- SAFFMAN, P. G. 1960 Dispersion due to molecular diffusion and macroscopic mixing in flow through a network of capillaries. *J. Fluid Mech.* **7**, 194–208.
- SHIRTCLIFFE, T. G. L. & TURNER, J. S. 1970 Observations of the cell structure of salt fingers. *J. Fluid Mech.* **41**, 707–719.
- STERN, M. E. & TURNER, J. S. 1969 Salt fingers and convecting layers. *Deep-Sea Res.* **16**, 497–511.
- TAUNTON, J. W., LIGHTFOOT, E. N. & GREEN, T. 1972 Thermohaline instability and salt fingers in a porous medium. *Phys. Fluids* **15**, 748–753.
- TAYLOR, J. & VERONIS, G. 1986 Experiments on salt fingers in a Hele-Shaw cell. *Science* **231**, 39–41.
- TODD, D. K. 1980 *Groundwater Hydrology*, 2nd edn, p. 82. Wiley.
- TURNER, J. S. 1985 Multicomponent convection. *Ann. Rev. Fluid Mech.* **17**, 11–44.
- TYVAND, P. A. 1980 Thermohaline instability in anisotropic porous media. *Water Resources Res.* **16**, 325–330.
- WEAST, R. C. (ed.) 1983 *CRC Handbook of Chemistry and Physics*, 64th edn, p. F-46. The Chemical Rubber Co.